J. Math. Kyoto Univ. (JMKYAZ)
23-1 (1983) 39-54

# Chaos and bifurcation phenomena in limitting central difference scheme

Dedicated to Professor Hisaaki Yoshizawa on his 60th birthday.

By

Masahiro MIZUTANI, Toshio NIWA and Taijiro OHNO

(Communicated by Prof. Yamaguti, Nov. 5, 1981)

## 0. Introduction.

It is known that solution of ordinary differential equation by means of central difference scheme does not lead one to the true solution but rather different solutions, so called ghost solutions. The significance of this phenomena was first recognized and analysed mathematically by M. Yamaguti and S. Ushiki [5, 6]. Mathematical mechanism of the appearance of the ghost solution in the 1-dimensional system was elucidated by Y. Takahashi [4]. In this note we consider the $n$-dimensional case ($n \geqslant 2$), and show that in general the solution by means of central difference scheme leads one to considerably different solutions, no matter how small one make the time mesh $\Delta t$, or even when one takes the limit $\Delta t \to 0$. We also show that limitting central difference scheme exhibits very interesting bifurcation phenomena when the original differential equation has a symmetry.

Let us consider an ordinary differential equation on $R^n$ (in general on an open domain of it).

$$\dot{x}=f(x), \quad x \in R^n \qquad \left( \cdot = \frac{d}{dt} \right) \tag{1}$$

The corresponding central difference equation is given by

$$\frac{x_{m+1}-x_{m-1}}{2\Delta t}=f(x_m), \quad x_m \in R^n \quad (\Delta t>0) \tag{2}$$

Does the solution of (2) approximates well the corresponding solution of (1)? It will be shown this is not the case even if we take the limit $\Delta t \to 0$ in the sense stated latter. We show the solution of (2) converges to the corresponding solution of the equation

$$\begin{aligned} \dot{x}&=f(y) \\ \dot{y}&=f(x) \end{aligned} \tag{3}$$

in the limit that $\Delta t \to 0$. This is veryfied in §1 in slightly more general situation.

More precisely, let $x_m(x_0, x_1; \Delta t)$ be a solution of (2) with the initial condition $x_0(x_0, x_1; \Delta t)=x_0$, and $x_1(x_0, x_1; \Delta t)=x_1$. If we set

$$x(t; \Delta t)=x_{2[t/\Delta t]}(x_0, x_1; \Delta t)$$

$$y(t; \Delta t)=x_{2[t/\Delta t]+1}(x_0, x_1; \Delta t)$$

(here $[r]$ denotes the integral part of the number $r$)
then the limits

$$\lim_{\Delta t\to 0} x(t; \Delta t)=x(t), \quad \lim_{\Delta t\to 0} y(t; \Delta t)=y(t)$$

exist, and $(x(t), y(t))$ is a solution of the equation (3) with the initial condition $(x(0), y(0))=(x_0, x_1)$.

We call the equation (3) the centralization of the equation (1). The centralization (3) is a consequence of an averaging of the equation (1) in the direction to the future and to the past in some sense.

Centralized equations have a number of remarkable properties.

Firstly, the diagonal $\Delta=\{(x, y)\in R^n\times R^n | x=y\}$ is an invariant space of (1), and the system on $\Delta$ is equivalent to the original equation (1). That is, centralized equation has a sub-system equivalent to the original equation. Secondly, centralized equation preserves the Lebesgue measure, that is, it induces a measure preserving flow. This follows from that the divergence of the right hand side of (3) vanishes.

Here we give the important remark, which follows from the facts stated above: If $x_0\in R^n$ is a stable point of the system (1) in the sense that $\operatorname{div} f(x_0)<0$, then the invariant manifold $\Delta$ of the system (3) is unstable at the corresponding point $(x_0, x_0)\in \Delta$, namely, the solution curves of the system (3) passing through the points $(\notin \Delta)$ near to $(x_0, x_0)$ leave exponentially from the $\Delta$. This means that if we approximate the system (1) by the system (2), then the error grows with exponential rate which is independent of small enough $\Delta t$. In this sense, the solutions of (2) do not approximate well the solutions of (1) no matter how small we make the time mesh $\Delta t$.

Especially, centralized equation is Hamiltonian, if and only if the original equation is a gradient system. Here, symplectic structure on $R^n\times R^n$ is given by the usual one $\omega^2=dx\wedge dy=\sum_i dx_i\wedge dy_i$, that is, $x$ and $y$ are the conjugate variables. This may be very interesting because of the contrasted properties of the gradient systems and the Hamiltonian systems. Note that 1-dimensional system is always a gradient system. "Centralization of the static system leads the metabolic system." If the original system is Hamiltonian, then the centralization of it is again Hamiltonian, where symplectic structure of the space $R^n\times R^n\ni(p, q; P, Q)$, $R^n=R^{2m}\ni(p, q)$ is not the natural one but one given by $\tilde{\omega}^2=dp\wedge dQ+dP\wedge dq$. Especially, if the original system is natural Hamiltonian, i.e. Hamiltonian with a Hamiltonian function

$$H(p, q)=T(p)+U(q),$$

then, centralization is given by

$$\dot{p}=-\frac{\partial U}{\partial Q}, \quad \dot{Q}=\frac{\partial T}{\partial p}, \quad \dot{P}=-\frac{\partial U}{\partial p}, \quad \dot{q}=\frac{\partial T}{\partial P},$$

that is, the sum of independent two identical systems which are equivalent to the original system. This means that if we project the solution of the centralization to the space $(p, Q)$ or $(P, q)$, then we get the true solution of the original system.

Similar situation occurs when one deal with the linear equation

$$\dot{x}=Ax.$$

Its centralization

$$\dot{x}=Ay, \ \dot{y}=Ax$$

is transformed to

$$\dot{X}=Ax, \ \dot{Y}=-AY,$$

if we set $X=x+y$ and $Y=x-y$.

In 3 we investigate some concrete example, which depends on a parameter and appears in the well known Hopf bifurcation:

$$\begin{aligned}\dot{x}_1&=x_1(1-(x_1^2+x_2^2))-\omega x_2\\ \dot{x}_2&=x_2(1-(x_1^2+x_2^2))+\omega x_1\end{aligned} \tag{4}$$

This system is invariant under the rotation arround the origin and is a gradient system when $\omega=0$.

Because of its rotational invariance, its centralization

$$\begin{aligned}\dot{x}_1&=y_1(1-(y_1^2+y_2^2))-\omega y_2\\ \dot{x}_2&=y_2(1-(y_1^2+y_2^2))+\omega y_1\\ \dot{y}_1&=x_1(1-(x_1^2+x_2^2))-\omega x_2\\ \dot{y}_2&=x_2(1-(x_1^2+x_2^2))+\omega x_1\end{aligned} \tag{5}$$

can be reduced to a 3-dimensional system. Especially, when $\omega=0$, it has a first integral, that is, kinetic momentum $F=x_1y_2-x_2y_1$, so the system is integrable.

If the original system (1) has not symmetries, then its centralization has, even if (1) is gradient system, very complicated structure and its solutions show chaotic behavior.

Returning to the system (4) and its centralization (5), when $\omega$ is large (say $\omega=1$) the solutions of the system (5) show the behavior similar to the 1-dimensional case. When $\omega$ is small (say $\omega=0.2$) it shows chaotic behavior. In other words, the one-parameter family of the system (5) has an interesting bifurcation phenomenon. To see this, let us consider the Poincaré map of the "periodic" solution ($\phi=\phi=0$, $\eta=2$, $\phi=\theta-\pi=0$, $\eta=0$) of the reduced system (6) of (5):

$$\dot{\eta}=\eta(2-\eta)\cos\phi\cos\theta$$

$$\dot{\phi}=2(\eta-1)\sin\phi\cos\theta-2\omega\sin\theta \tag{6}$$

$$\dot{\theta}=\frac{1}{\cos\phi}\left[\{\eta(1+\sin^2\phi)-2\}\sin\theta+2\omega\sin\phi\cos\theta\right]$$

According to a detailed analysis by a computer, when $\omega=1$, the Poincaré map is as a fig. 4, which is well known as a first approximation (or an averaging) of a perturbed twist mapping (cf. Henon and Heiles [3]), when $\omega=0.554$ the mixture of the invariant circles and instability zones which are very thin, which appear in the perturbed twist mapping in general (see fig. 5). When $\omega=0.548$ the instability zones grow and show a chaotic behavior (see fig. 6).

Lastly, we should note that the centralization of the system depends unfortunately on the coordinate systems in general. As is easily seen, the centralization procedure is compatible only with the affine transformation of the space $R^n$.

## 1. Centralization of differential equations.

Let

$$\dot{x}=f(x), \quad x\in R^n \tag{1}$$

be a differential equation on an $n$-dimensional space $R^n$.

Let

$$\frac{x_{m+1}-x_{m-1}}{2\Delta t}=f(x_m), \quad x_m\in R^n, \quad \Delta t>0 \tag{2}$$

be the corresponding central difference equation. If we put $y_m=x_{m+1}$, then (2) can be rewritten to the form

$$\begin{aligned} x_{m+2}-x_m&=\varepsilon\, f(y_m) \\ y_{m+2}-y_m&=\varepsilon\, f(x_m+\varepsilon\, f(y_m)) \end{aligned} \tag{2$'$}$$

where $\varepsilon=2\Delta t>0$.

We show that solutions of (2)$'$ converge to the corresponding solutions of the equation

$$\begin{aligned} \dot{x}&=f(y) \\ \dot{y}&=f(x) \end{aligned} \tag{3}$$

in the sense stated in the introduction. We prove it in more general form.

**Definition.** Let $\{\phi_t\}$ be a smooth (local) flow defined on a smooth manifold $M$. Let $\{\Phi_s\}$ be a family of smooth mappings of $M$ which satisfy the following conditions:

(i) $\Phi_0=id.$

(ii) $\frac{d}{dt}(\phi_t(x))|_{t=0}=\frac{d}{ds}(\Phi_s(x))|_{s=0}$

We call such a family $\{\Phi_s\}$ a discretization of the local flow $\{\phi_t\}$.

**Theorem 1.** *Let $\{\phi_t\}$, $\{\Phi_s\}$ be as above. Let $(T, x_0)$ be in the domain of the flow $\phi_t(x)$, and $\Delta$ be a decompotion of the interval $[0, T]$; $0=t_0<t_1<\cdots<t_N=T$, $|\Delta|=\max(t_{i+1}-t_i)$, then if $|\Delta|$ is sufficiently small*

$$\Big(\prod_{i=0}^{N-1} \Phi_{t_{i+1}-t_i}\Big)(x_0)$$

*is defined, and converges to $\phi_T(x_0)$: $\phi_T(x_0)=\lim_{|\Delta|\to 0}\big(\prod \Phi_{t_{i+1}-t_i}\big)(x_0)$*

**Remark.** This result can be easily extended to the time dependent flow.

*Proof.* It is clear that there exists a neighborhood $U$ of $\{(x, t)\in M\times R;\ x=\phi_t(x_0),\ 0\leqslant t\leqslant T\}$ in the extended phase space $M\times R$ of the flow $\{\phi_t\}$ such that:

(i) if $(x, t)\in U$, then $\phi_s(x)\in U$ for $-t\leqslant s\leqslant T-t$

(ii) if $(x, t)\in U$, then there exist $\varepsilon>0$, $K_1>0$ such that $\Phi_s(x)$ is defined for $|s|<\varepsilon$, and $\rho(\phi_s(x), \Phi_s(x))<K_1|s|^2$ (here $\rho$ is a metric of $M$)

(iii) $\phi_t(x)$ is Lipschitz continuous, that is, there exists $K_2>0$ such that if $(x, t)$, $(y, t)\in U$ then $\rho(\phi_s(x), \phi_s(y))<e^{K_2|s|}\rho(x, y)$ for $-t\leqslant s\leqslant T-t$.

Now let

$$x_k=\prod_{i=1}^{k}\Phi_{t_i-t_{i-1}}(x_0),\quad k=0, 1,\ldots, N.$$

we show inductively that $(x_k, t_k)\in U$ if $|\Delta|$ is sufficiently small. Assume that $(x_k, t_k)\in U$ and

$$\rho(\phi_{T-t_k}(x_k), \phi_T(x_0))\leqslant e^{K_2T}K_1\sum_{i=1}^{k}(t_i-t_{i-1})^2$$

then

$$\begin{aligned}
\rho(\phi_{T-t_{k+1}}(x_{k+1}), \phi_T(x_0)) &= \rho(\phi_{T-t_{k+1}}(\Phi_{t_{k+1}-t_k}(x_k)), \phi_T(x_0))\\
&\leqslant \rho(\phi_{T-t_{k+1}}(\Phi_{t_{k+1}-t_k}(x_k)), \phi_{T-t_{k+1}}(\phi_{t_{k+1}-t_k}(x_k))+\rho(\phi_{T-t_k}(x_k), \phi_T(x_0))\\
&\leqslant e^{K_2(T-t_{k+1})}\rho(\Phi_{t_{k+1}-t_k}(x_k),\ \phi_{t_{k+1}-t_k}(x_k))+e^{K_2T}K_1\sum_{i=1}^{k}(t_i-t_{i-1})^2\\
&\leqslant e^{K_2T}K_1(t_{k+1}-t_k)^2+e^{K_2T}K_1\sum_{i=1}^{k}(t_i-t_{i-1})^2\\
&= e^{K_2T}K_1\sum_{i=1}^{k+1}(t_i-t_{i-1})^2<e^{K_2T}K_1|\Delta|T.
\end{aligned}$$

Hence, if $|\Delta|$ is sufficiently small, then $(\phi_{T-t_{k+1}}(x_{k+1}), T)\in U$ so $(x_{k+1}, t_{k+1})\in U$.

Therefore, $\rho(x_N, \phi_T(x))\leqslant e^{K_2T}K_1|\Delta|T$, that is,

$$\rho\Big(\prod_{i=0}^{N-1}\Phi_{t_{i+1}-t_i}(x_0), \phi_T(x)\Big)\leqslant K_1Te^{K_2T}|\Delta|$$

Hence,

$$\lim_{|\Delta|\to 0}\left(\prod_{i=0}^{N-1}\Phi_{t_{i+1}-t_i}\right)(x_0)=\phi_T(x_0). \qquad \text{Q.E.D.}$$

Convergence of the system (2) to the (3) is clear from this theorem 1;

Let $(x_{n+2}, y_{n+2})=\Phi_\varepsilon(x_n, y_n)\equiv(x_n+\varepsilon f(y_n), y_n+\varepsilon f(x_n+\varepsilon f(y_n)))$ then $\frac{d}{d\varepsilon}\Phi_\varepsilon(x_n, y_n)_{|\varepsilon=0}=(f(y_n), f(x_n))$.

**2. Centralization and Hamiltonian system.**

In this section we study the relation between a system (1) and its centralization (3).

**Theorem 2.** *The centralized system* (3) *is a Hamiltonian system with the natural symplectic structure of* $R^n\times R^n$, $\omega^2=dx\wedge dy=\sum dx_i\wedge dy_i$, *iff the system* (1) *is a gradient system.*

*Proof.* Let (1) be a gradient system, i.e.

$$\dot{x}=\operatorname{grad} U(x) \qquad \text{for some function } U(x) \text{ on } R^n.$$

Then (2) is given by

$$\dot{x}=-\frac{\partial H}{\partial y}, \quad \dot{y}=\frac{\partial H}{\partial x}, \quad \text{where } H(x, y)=U(x)-U(y).$$

Conversely, let (2) be a Hamiltonian system.
Let $X(x, y)=f(y)\frac{\partial}{\partial x}+f(x)\frac{\partial}{\partial y}$.
Then $i_X\omega=f(y)dy-f(x)dx$ is a closed form, so

$$di_X\omega=d(f(y)dy)-d(f(x)dx)=0,$$

that is, $d(f(x)dx)=0$. Therefore by the Poincaré's lemma, there exists a function $U(x)$ such that $f(x)dx=dU$, that is, $f(x)=\operatorname{grad} U(x)$. Q.E.D.

**Theorem 3.** *Let the system* (1) *be a Hamiltonian system*:

$$\begin{gathered}\dot{p}=-\frac{\partial H}{\partial q}, \quad \dot{q}=\frac{\partial H}{\partial p}, \quad H=H(p, q)\\ x=(p, q)\in R^m\times R^m=R^{2m}\end{gathered} \tag{7}$$

*then its centralization*

$$\begin{gathered}\dot{p}=-\frac{\partial H}{\partial q}(P, Q), \quad \dot{q}=\frac{\partial H}{\partial p}(P, Q)\\ \dot{P}=-\frac{\partial H}{\partial q}(p, q), \quad \dot{Q}=\frac{\partial H}{\partial p}(p, q)\\ y=(P, Q)\in R^m\times R^m\end{gathered} \tag{8}$$

*is again a Hamiltonian system with the Hamiltonian function*

$$\tilde{H}(p, q, P, Q)=H(p, q)+H(P, Q)$$

*and the symplectic structure* $\tilde{\omega}^2$ *on* $(R^m \times R^m)\times(R^m \times R^m)$

$$\tilde{\omega}^2=dP\wedge dq+dp\wedge dQ.$$

**Remark.** If the Hamiltonian system (7) is a natural one, i.e.

$$H(p, q)=T(p)+U(q)$$

then (8) is given by

$$\dot{P}=-\frac{\partial H(P, q)}{\partial q}, \quad \dot{q}=\frac{\partial H(P, q)}{\partial P}$$

$$\dot{p}=-\frac{\partial H(p, Q)}{\partial Q}, \quad \dot{Q}=\frac{\partial H(p, Q)}{\partial p}$$

That is, the sum of two independent systems which are same as the original system (7).

The proof of the theorem 3 is straightforward.

### 3. Centralization and Bifurcation.

Let us consider the following system (4) and its centralization (5):

$$\begin{cases} \dot{x}_1=x_1(1-(x_1^2+x_2^2))-\omega x_2 \\ \dot{x}_2=x_2(1-(x_1^2+x_2^2))+\omega x_1, \ x=(x_1, x_2)\in R^2 \end{cases} \tag{4}$$

$$\begin{cases} \dot{x}_1=y_1(1-(y_1^2+y_2^2))-\omega y_2 \\ \dot{x}_2=y_2(1-(y_1^2+y_2^2))+\omega y_1 \\ \dot{y}_1=x_1(1-(x_1^2+x_2^2))-\omega x_2 \\ \dot{y}_2=x_2(1-(x_1^2+x_2^2))+\omega x_1, \ (x, y)=(x_1, x_2, y_1, y_2)\in R^2\times R^2 \end{cases} \tag{5}$$

Because of the rotational invariance of the system (5), (5) can be reduced to a 3-dimensional system.

Let $\quad x_1=r\cos\alpha,\ x_2=r\sin\alpha \quad (r\geqslant 0)$

$\quad y_1=s\cos\beta,\ y_2=s\sin\beta \quad (s\geqslant 0)$

and let

$$r=\sqrt{\eta}\cos\left(\frac{\phi}{2}+\frac{\pi}{4}\right),\ s=\sqrt{\eta}\sin\left(\frac{\phi}{2}+\frac{\pi}{4}\right)$$

$$\theta=\alpha-\beta \tag{7}$$

$$\eta\geqslant 0,\ -\frac{\pi}{2}\leqslant\phi\leqslant\frac{\pi}{2}, \quad \theta \ (\mathrm{mod}\ 2)$$

Then (5) is reduced to the system,

$$\begin{aligned}
\dot{\eta} &= \eta(2-\eta)\cos\phi\cos\theta \\
\dot{\phi} &= 2(\eta-1)\sin\phi\cos\theta - 2\omega\sin\theta \\
\dot{\theta} &= \frac{1}{\cos\phi}\{(\eta(1+\sin^2\phi)-2)\sin\theta + 2\omega\sin\phi\cos\theta\}
\end{aligned} \tag{6}$$

The system (5) or (6) has several special properties:

(i) When $\omega=0$, (5) is a Hamiltonian system with Hamiltonian

$$H(x, y) = \frac{1}{2}(x_1^2+x_2^2) - \frac{1}{4}(x_1^2+x_2^2)^2 - \frac{1}{2}(y_1^2+y_2^2) + \frac{1}{4}(y_1^2+y_2^2)^2$$

Because of its rotational symmetry, it has an integral, so called angular momentum $F(x, y) = x_2y_1 - x_1y_2$. Therefore the system (5) is completely Integrable, so we can study it thoroughly (cf. V. Arnold [1]).

(ii) The system (6) is invariant under the following transformations:

(a) $(\eta, \phi, \theta) \longmapsto (\eta, -\phi, -\theta)$

(b) $(\eta, \phi, \theta) \longmapsto (\eta, \phi, \theta+\pi)$ with $t \longmapsto -t$

(iii) $S_0=\{\eta=0\}$, and $S_2=\{\eta=2\}$ are invariant surfaces so $\bar{D}=\{0\leqslant\eta\leqslant 2\}$ is an invariant domain of the system (5). $\{\phi=0, \theta=0, 0<\eta<2\}$ and $\{\phi=0, \theta=\pi, 0<\eta<2\}$ are solution curves of the system.

Henceforth we consider the system (6) in the invariant domain $\bar{D}=\{0\leqslant\eta\leqslant 2\}$, $\partial\bar{D}=S_0\cup S_2$, $D=\bar{D}-\partial\bar{D}$, especially near the solution, $\phi=\theta=0$, $0<\eta<2$, which correspondings to the solution with the initial condition $x=y$ of the system (5).

First, we consider the case $\omega=0$:

As is mentioned,

$$H(\eta, \phi, \theta) = \frac{1}{4}\eta(\eta-2)\sin\phi$$

$$F(\eta, \phi, \theta) = \frac{1}{2}\eta\cos\phi\sin\theta$$

are integrals of the system (5) with $\omega=0$.

Now,

$$\operatorname{grad} H \equiv \left(\frac{\partial H}{\partial\eta}, \frac{\partial H}{\partial\phi}, \frac{\partial H}{\partial\theta}\right) = \frac{1}{4}(2(\eta-1)\sin\phi, \eta(\eta-2)\cos\phi, 0)$$

$$\operatorname{grad} F = \frac{1}{2}(\cos\phi\sin\theta, -\eta\sin\phi\sin\theta, \eta\cos\phi\cos\theta)$$

In the invariant domain $D=\{0<\eta<2\}$, grad $H$ and grad $F$ are not linearly independent on the set

$$\left\{(\eta, \phi, \theta) | \eta=1, \phi=\pm\frac{\pi}{2}\right\} \cup \left\{(\eta, \phi, \theta) | \phi=\pm\frac{\pi}{2}, \theta=n\pi\right\} \cup$$

$$\cup \left\{(\eta, \phi, \theta) | \eta = \frac{2}{1+\sin^2\phi}, \phi = 0, \pm\frac{\pi}{2}, \theta = \frac{\pi}{2} + n\pi\right\}$$

Taking these circumstances into consideration, we can see that almost all solutions are periodic. Especially, orbits which start from near the solution $\phi=\theta=0$ are all periodic except ones on the surface $\phi=0$ or $\theta=0$ (see fig. a).

Let us turn to the case $\omega \neq 0$.

At first, we consider the system (6) on the invariant surface $S_2$. On $S_2$ (6) becomes

$$\begin{aligned} \dot{\phi} &= 2(\sin\phi\cos\theta - \omega\sin\theta) \\ \dot{\theta} &= 2\frac{\sin\phi}{\cos\phi}(\sin\phi\sin\theta + \omega\cos\theta) \end{aligned} \tag{8}$$

Fixed points of this system are $(\phi, \theta)=(0, 0)$ and $(0, \pi)$. And the linearlized system of it around $(0, 0)$ is given by

$$\frac{d}{dt}\begin{pmatrix} \phi \\ \theta \end{pmatrix} = \begin{pmatrix} 2 & -2\omega \\ 2\omega & 0 \end{pmatrix}\begin{pmatrix} \phi \\ \theta \end{pmatrix}$$

and its eigenvalues are $\lambda = 1 \pm \sqrt{1-4\omega^2}$.

Taking its symmetries (7) into consideration, we can draw the phase portrait of the system (8) on $S_2$ (see fig. b, c)

Similarly, on the invariant surface $S_0$ (6) becomes

$$\begin{aligned} \dot{\phi} &= -2(\sin\phi\cos\theta + \omega\sin\theta) \\ \dot{\theta} &= \frac{-2}{\cos\phi}(\sin\theta - \omega\sin\phi\cos\theta) \end{aligned} \tag{9}$$

Fixed points of this system are $(\phi, \theta)=(0, 0)$ and $(0, \pi)$. Linearlized system arround $(0, 0)$ is given by

$$\frac{d}{dt}\begin{pmatrix} \phi \\ \theta \end{pmatrix} = \begin{pmatrix} -2 & -2\omega \\ 2\omega & -2 \end{pmatrix}\begin{pmatrix} \phi \\ \theta \end{pmatrix}$$

and its eigenvalues are $\lambda = -2 \pm 2\omega i$

The phase portrait of the system (9) is shown in fig. d, e.

Next, we investigate the system (5) near the solution $\phi=\theta=0$. In order that we consider the variational equation along the solution $\phi=\theta=0$, $\dot{\eta}=\eta(2-\eta)$:

$$\frac{d}{dt}\begin{pmatrix} \partial\eta \\ \partial\phi \\ \partial\theta \end{pmatrix} = \begin{pmatrix} 2(1-\eta) & 0 & 0 \\ 0 & 2(\eta-1) & -2\omega \\ 0 & 2\omega & \eta-2 \end{pmatrix}\begin{pmatrix} \partial\eta \\ \partial\phi \\ \partial\theta \end{pmatrix}, \quad \eta=\eta(t) \tag{10}$$

If $\partial\eta(0)=0$, then $\partial\eta(t)\equiv 0$. This means planes that are perpendicular to the solution line $\phi=\theta=0$ are preserved by the variational equation (10). The variational equation (10) can, therefore, be seen as a time dependent 2-dimensional system:

$$\frac{d}{dt}\begin{pmatrix} \partial\phi \\ \partial\theta \end{pmatrix} = \begin{pmatrix} 2(\eta-1) & -2\omega \\ 2\omega & \eta-2 \end{pmatrix}\begin{pmatrix} \partial\phi \\ \partial\theta \end{pmatrix} \qquad , \ \eta=\eta(t)$$

Let

$$A(\eta)=\begin{pmatrix} 2(\eta-1) & -2\omega \\ 2\omega & \eta-2 \end{pmatrix}$$

The eigenvalues of $A(\eta)$ are $\lambda=\frac{1}{2}(3\eta-4\pm\sqrt{\eta^2-16\omega^2})$

If $\omega$ is small enough, the system is of saddle type. $\phi=0$ is almost "stable" manifold, and $\theta=0$ is almost "unstable" manifold. Therefore, we can guess that "periodic" solution: $\phi=\theta=0$, $\eta=2$, $\phi=\theta-\pi=0$, $\eta=0$ is unstable. (Note the symmetry (7).) (see fig. g and fig. 3 drawn by computer)

Conversely, if $\omega$ is large, $\lambda$ are not real, so the behavior of the solutions of (6) near $\phi=\theta=0$ are resemble to the spiral, and the "periodic" solution can be stable. This expectation can be confirmed by the computation by computer. We can investigate the behavior of the solutions near the "periodic" one $\phi=\theta=0$, $\eta=2$, $\phi=\theta-\pi=0$, and $\eta=0$, by the Poincaré map. For this sake, take a cross section $S=\{(\eta, \phi, \theta) | \eta=0.6\}$, and the Poincaré map $P: S\to S$.

Unfortunately, we could not study it (mathematically) rigorously. By the detailed study by the computer analysis we can see that these Poincaré maps $P_\omega$ depending on a parameter $\omega$, show very interesting bifurcation phenomenon. For $\omega=1$, $P_1$ is "integrable", which appears in the first approximation or the averaging of the perturbed twist map (see Henon and Heiles [3] & fig. 4). For $\omega=0.554$, we can see the mixture of invariant circles and very thin instability zones. (see fig. 5) For $\omega=0.548$, chaotic region is already large. (see fig. 6)

**Acknowledgments**

The authors would like to thank Dr. A. Ichimura of Waseda University for his continuous encouragement and fruitful discussions on the numerical works and Prof. M. Yamaguti for his valuable comments.

DEPARTMENT OF APPLIED PHYSICS,
WASEDA UNIVERSITY
DEPARTMENT OF MATHEMATICS,
TSUDA COLLEGE
B.S.C., SHINBASHI, MINATOKU,
TOKYO

## References

[1] V. I. Arnold, Mathematical methods of classical mechanics, Springer-Verlag, New York, 1978.

[2] V. I. Arnold and A. Aves, Problèmes ergodiques de la mécanique classique, Gauthier-Villars, Paris, 1967.

[3] M. Henon and C. Heiles, The applicability of the third integral of motion: some numerical experiments, Astron. J. **69** (1964), 73–79.

[4] Y. Takahashi, A note of the ghost solutions of differential equations, to appear.

[5] M. Yamaguti and S. Ushiki, Chaos in numerical analysis of ordinary differential equations, to appear.

[6] ———, Discretisation et chaos, C. R. Acad. Paris, t. 290 (14 avril 1980), Serie A-637.

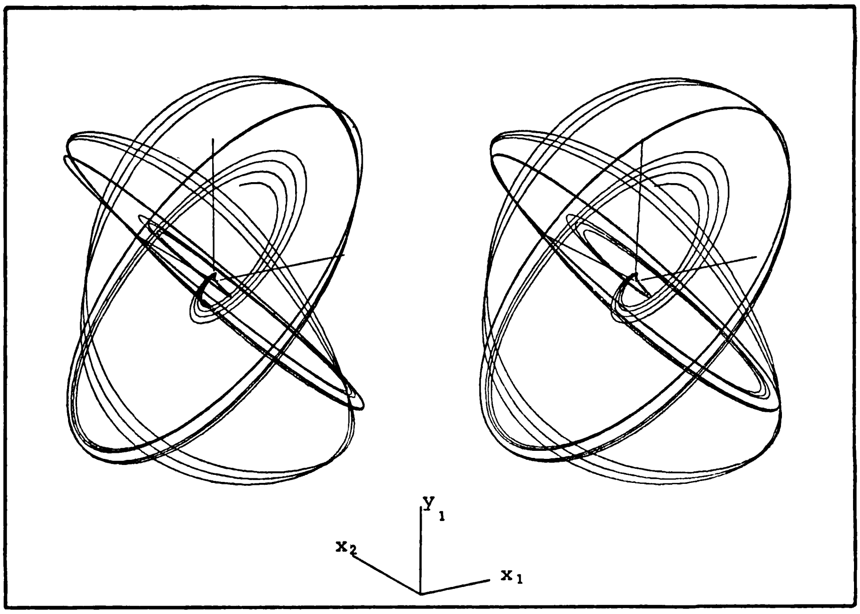


Fig. 1(a). Stereoplot of trajectorial flow of eq. (5) in the $(x_1, x_2, y_1)$ subspace. $\omega=1.0$. Initial values: $x_1(0)=0.031821658$, $x_2(0)=0.07054278$, $y_1(0)=0.031649066$, $y_2(0)=0.054817789$. (These values correspond to the initial values of Fig. 3 (a), (c).) Time 70. axes: 0,..., 1 for $x_1$, 0,..., 1 for $x_2$, 0,..., 1 for $y_1$. Initial values and axes of (b) are common to (a).

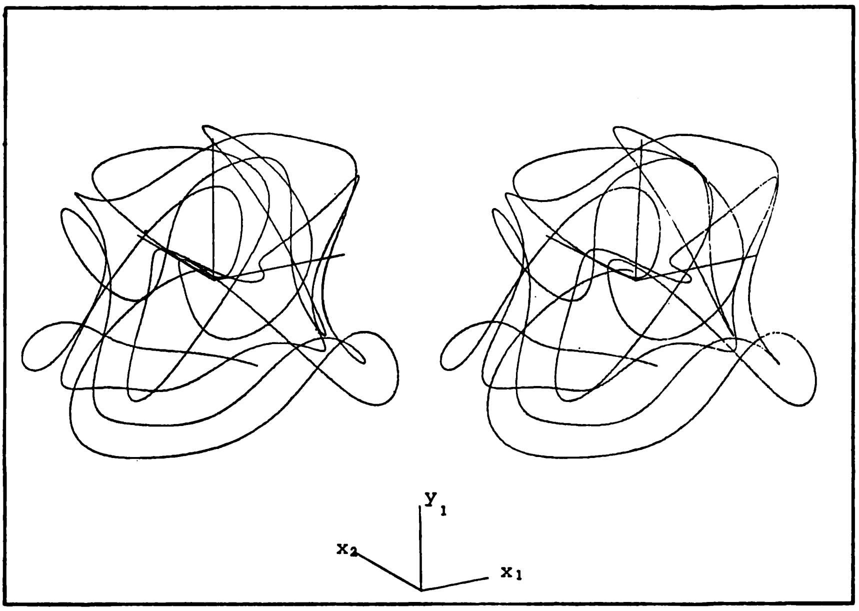


Fig. 1(b). $\omega=0.2$. Time 90.

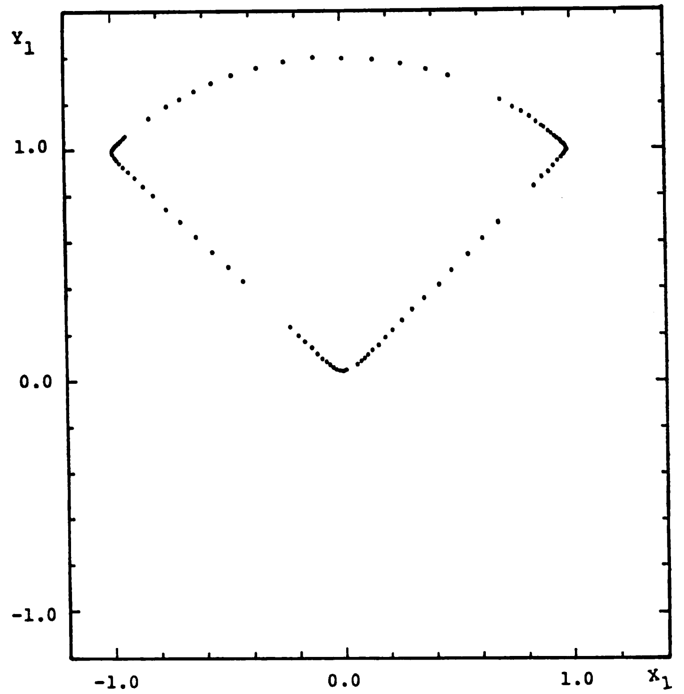


Fig. 2(a). Cross section of a trajectory of Fig. 1 with the $(x_1, y_1)$ plane. $\omega=1.0$. Time 350. Surface of section is determined by the conditions $x_2=0.0$ and $\dot{x}_2\geq 0$. This conditions are common to (b). Succesive points lie on a smooth curve.

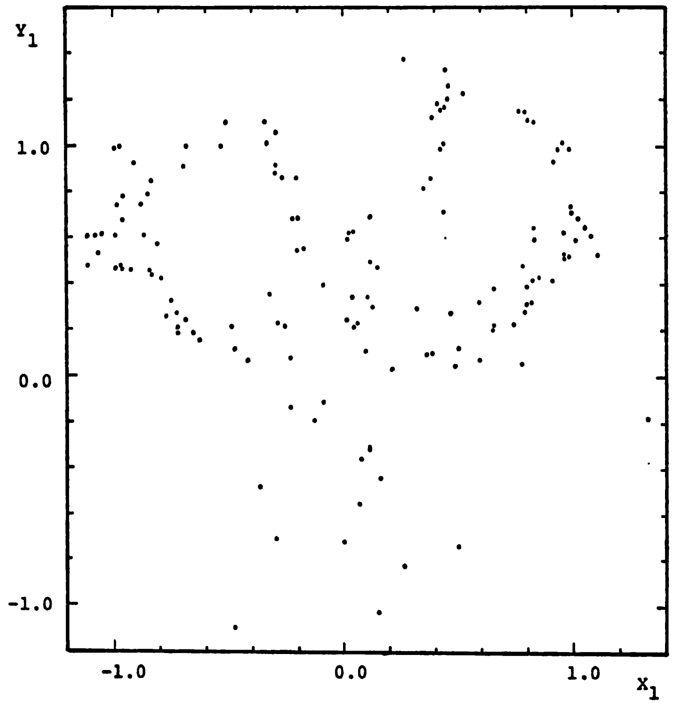


Fig. 2(b). $\omega=0.2$. Time 1500. Succesive points are scattered chaotically.

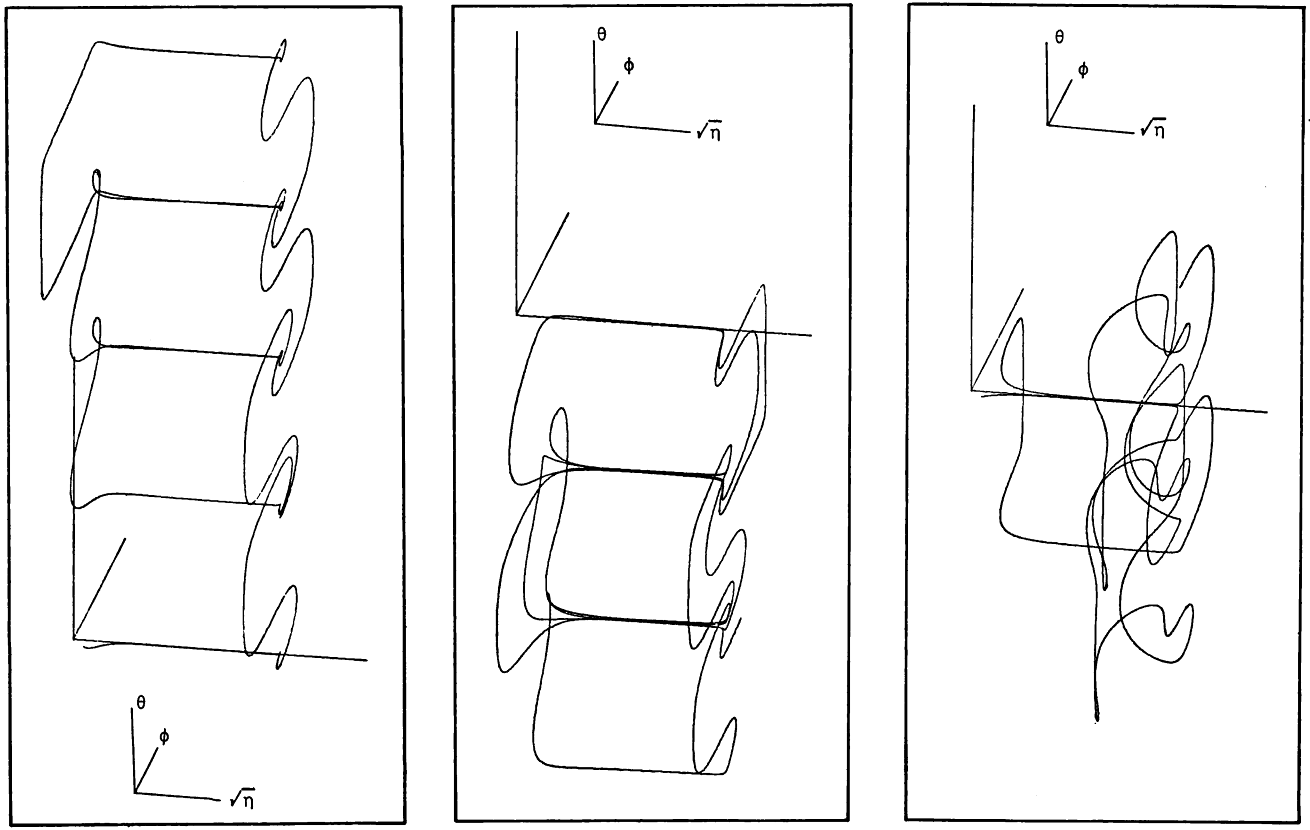


Fig. 3(a) Fig. 3(b) Fig. 3(c)

Fig. 3. (a) Trajectorial flow of eq. (6) in the $(\sqrt{\eta}, \phi, \theta)$ space. $\omega=1.0$. Time 80. Initial values: $\eta(0)=0.6$, $\phi(0)=-0.2$, $\theta(0)=0.1$. Axes: 0,..., 2 for $\sqrt{\eta}$, 0,..., 2 for $\phi$, 0,..., 6 for $\theta$. Time and axes of (b), (c) are common to (a). Figure (a) suggests the periodicity of a trajectory. (b). $\omega=0.55$. Initial values: $\eta(0)=0.6$, $\phi(0)=0.0$, $\theta(0)=0.01$. (c). $\omega=0.2$. Initial values: same as (a). The trajectory already loses the periodicity and behaves chaotically. (cf. Fig. 4, 5, 6.)

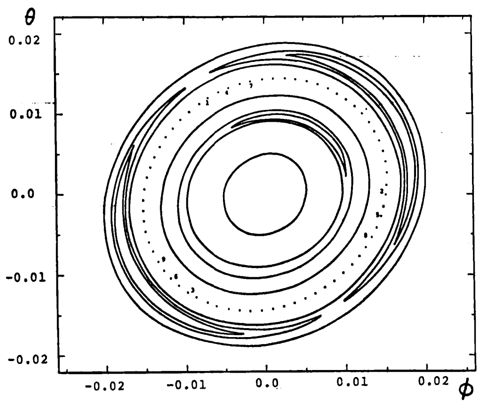


Fig. 4. Cross section of trajectories of eq. (6) with the ($\phi$, $\theta$) plane. $\omega=1.0$. Time 2000. Surface of section is determined by the conditions $\eta=0.6$ and $\dot{\eta}\geq 0$. This conditions and time are common to Fig. 5, 6. The microscopic instability zones lie below the computer integration accuracy. Here and in all level curves are drawn by real lines whenever intersection points of a trajectory obviously lie on a smooth curve. Points in this figure lie on a smooth curve and the number 1, 2, 3, .. indicates the order of succesive intersection points of a torajectory.

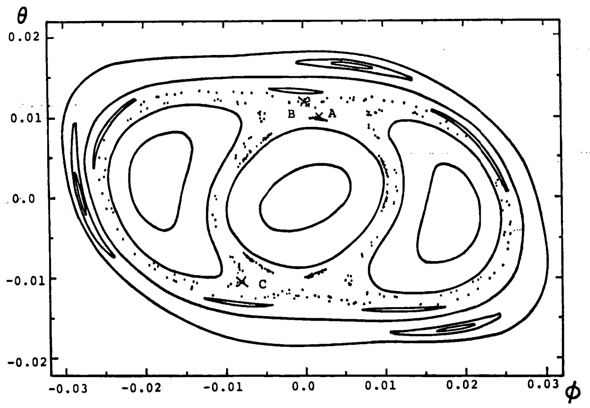


Fig. 5. Cross section of trajectories. $\omega=0.554$. In this stage, the instability zones grow visibly and islands are observed. Succesive points started from point A and C are surrounded by points started from point B.

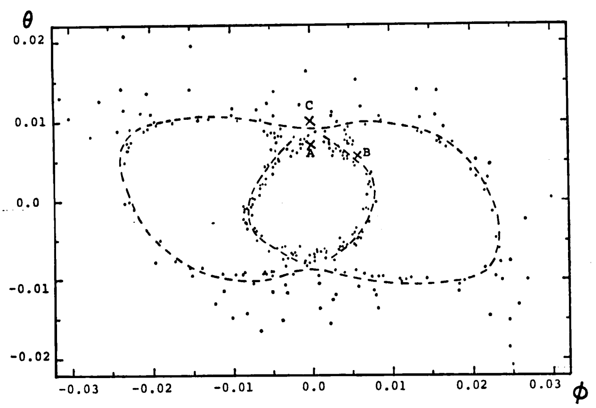


Fig. 6. Cross section of trajectories. $\omega=0.548$. Dotted lines distinguish the succesive points started from point A, B and C each other. Note: Instability zones grow rapidly as $\omega$ decreases.

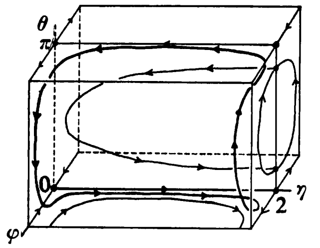


Fig. a

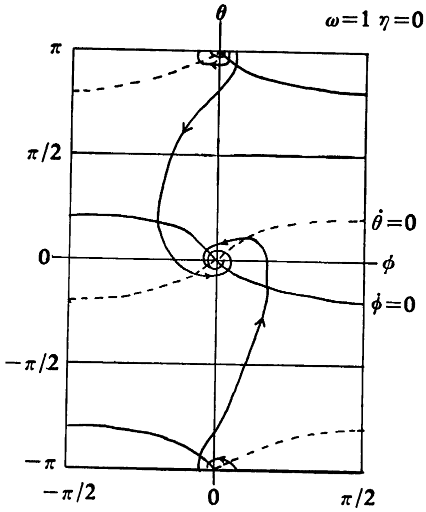


Fig. d

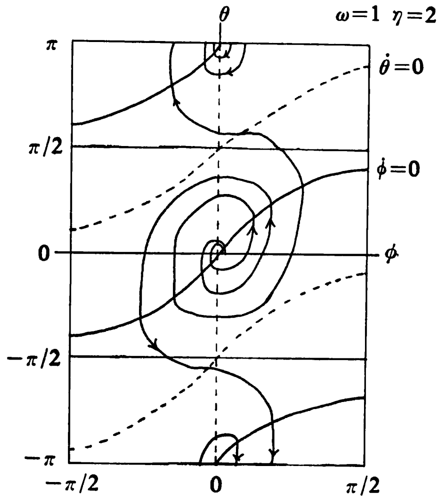


Fig. b

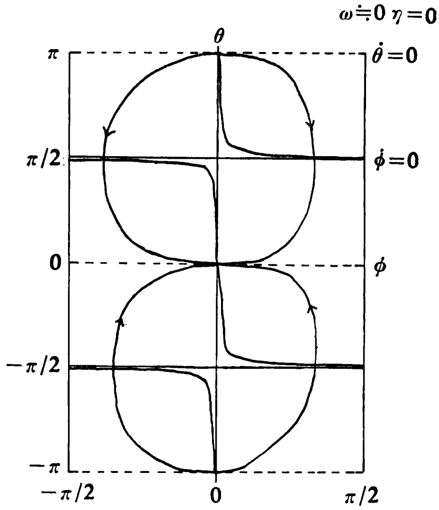


Fig. e

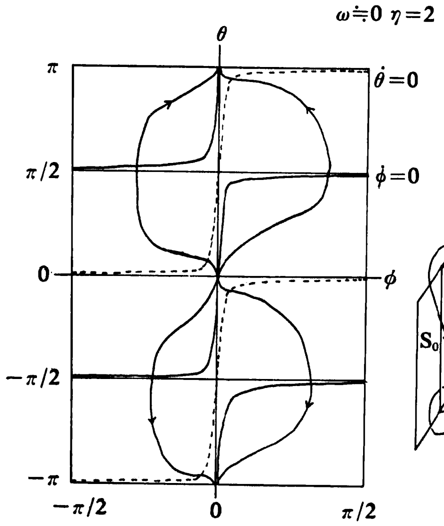


Fig. c

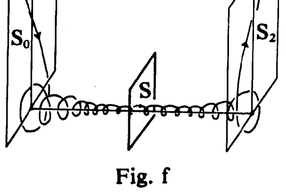


Fig. f

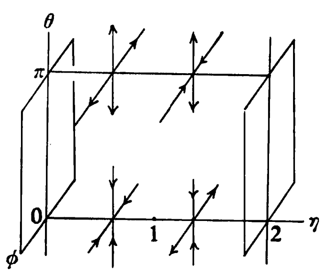


Fig. g